Published in final edited form as:

Biochim Biophys Acta. 2015 February ; 1853(2): 276–284. doi:10.1016/j.bbamcr.2014.11.015.

H9c2 and HL-1 cells demonstrate distinct features of energy metabolism, mitochondrial function and sensitivity to hypoxia-reoxygenation

Andrey V. Kuznetsov[a,*], **Sabzali Javadov**[b], **Stephan Sickinger**[a], **Sandra Frotschnig**[a], and **Michael Grimm**[a]

[a]Cardiac Surgery Research Laboratory, Department of Cardiac Surgery, Innsbruck Medical University, Innsbruck A-6020, Austria

[b]Department of Physiology, School of Medicine, University of Puerto Rico, San Juan, PR 00936-5067, USA

Abstract

Dysfunction of cardiac energy metabolism plays a critical role in many cardiac diseases, including heart failure, myocardial infarction and ischemia–reperfusion injury and organ transplantation. The characteristics of these diseases can be elucidated in vivo, though animal-free in vitro experiments, with primary adult or neonatal cardiomyocytes, the rat ventricular H9c2 cell line or the mouse atrial HL-1 cells, providing intriguing experimental alternatives. Currently, it is not clear how H9c2 and HL-1 cells mimic the responses of primary cardiomyocytes to hypoxia and oxidative stress. In the present study, we show that H9c2 cells are more similar to primary cardiomyocytes than HL-1 cells with regard to energy metabolism patterns, such as cellular ATP levels, bioenergetics, metabolism, function and morphology of mitochondria. In contrast to HL-1, H9c2 cells possess beta-tubulin II, a mitochondrial isoform of tubulin that plays an important role in mitochondrial function and regulation. We demonstrate that H9c2 cells are significantly more sensitive to hypoxia-reoxygenation injury in terms of loss of cell viability and mitochondrial respiration, whereas HL-1 cells were more resistant to hypoxia as evidenced by their relative stability. In comparison to HL-1 cells, H9c2 cells exhibit a higher phosphorylation (activation) state of AMP-activated protein kinase, but lower peroxisome proliferator-activated receptor gamma coactivator 1-alpha levels, suggesting that each cell type is characterized by distinct regulation of mitochondrial biogenesis. Our results provide evidence that H9c2 cardiomyoblasts are more energetically similar to primary cardiomyocytes than are atrial HL-1 cells. H9c2 cells can be successfully used as an in vitro model to simulate cardiac ischemia–reperfusion injury.

[*]Corresponding author at: Cardiac Surgery Research Laboratory, Department of Cardiac Surgery, Innsbruck Medical University, Innrain 66, A-6020 Innsbruck, Austria. Tel.: +43 512 504 27815; fax: +43 512 504 24625. andrey.kuznetsov@uki.at (A.V. Kuznetsov).

Disclosures

No confiicts of interest, financial or otherwise, are declared by the authors.

Keywords

Energy metabolism; H9c2 cells; HL-1 cells; Hypoxia-reoxygenation; Mitochondria

1. Introduction

Ischemia–reperfusion (IR) injury mechanisms are complex and numerous. They include disruption of ionic homeostasis, in particular calcium, mitochondrial permeability transition, energetic and oxidative stresses, induction of cell death by apoptosis, and necrosis [1–5]. Indeed, existing studies show that cardiac dysfunction can be directly linked to mitochondrial damage and depressed cellular energy metabolism [5–7]. Many aspects of cardiac IR injury are not yet fully understood. In addition to organ models, like coronary artery occlusion, the ex vivo model of IR, cold storage, and organ transplantation, cell in vitro models are used to simulate cardiac IR injury. These models entail the use of cultured neonatal/adult cardiomyocytes [8–11], mouse atrial HL-1 cells, or rat ventricular H9c2 cells (myoblasts) [12–20]. Neonatal cardiomyocytes can be considered as a very useful model for cardiac ventricular cells, in particular to study various adaptive mechanisms. This model represents a homogeneous population of cardiac cells, offering numerous experiments to simulate cardiac pathologies. However, the absence of mitochondrial creatine kinase and increased levels/activity of membrane-bound hexokinase allow assuming that neonatal cells are more dependent on glucose and possess more glycolytic phenotype as compared with adult cardiomyocytes. Hearts of fetal and newborn mammalians therefore are more dependent on glycolysis, whereas adult hearts are almost exclusively aerobic and mainly utilize free fatty acids [21]. As a consequence, neonatal hearts are rather resistant to hypoxia. Moreover, shortly after birth, cardiac cells lose their ability to divide.

Both H9c2 and HL-1 cell lines are immortalized cells with a cardiac phenotype, and both are widely used for the analysis of cardiac IR injury and ischemic preconditioning [22]. Currently, the experimental outcomes of studies using these unique cell lines and their interpretations suggest significant differences between them. Although existing data provide some indications that H9c2 cells can be a better model [6,23], direct comparative studies of the main bioenergetic parameters of H9c2 and HL-1 cell lines, under normal conditions and in response to hypoxia and oxidative stress, are still missing. Therefore, the aim of the study was compare the most important energy-related characteristics of H9c2 and HL-1 cell lines. It has been previously shown that the bioenergetic patterns and metabolic and functional properties of HL-1 cells are significantly different from those of primary adult cardiomyocytes. Some of these differences involve energy status and key parameters of mitochondrial respiratory regulation, such as apparent Km for ADP, the roles of creatine kinase system, and hexokinase [24–26]. Our study compares the most important energy-related characteristics of H9c2 and HL-1 cells, such as ATP levels, mitochondrial biogenesis, morphology, interaction of mitochondria with cytoskeleton, respiration of mitochondria, and sensitivity of the cells to hypoxia-reoxygenation, by using mitochondrial confocal imaging, enzymatic and high-resolution respirometry approaches.

AMP activated protein kinase (AMPK) and peroxisome proliferator-activated receptor (PPAR) gamma coactivator 1-alpha (PGC-1α) are among the most important signaling

proteins in mitochondrial biogenesis and oxidative function. Therefore, in addition to mitochondrial morphology, biogenesis and function, we investigated protein levels of AMPK, P-AMPK and PGC-1α during basal conditions, hypoxia alone, and hypoxia-reoxygenation. AMPK plays a key role as an energy sensor in the cell; energetic stressors change the AMP/ATP ratio, stimulating AMPK to regulate a variety of metabolic processes and pathways, like glycolysis, glucose uptake (GLUT4 translocation) and fatty acid oxidation [27]. PGC-1α is a key regulator of the mitochondrial transcriptional network. It co-activates PPARs to upregulate fatty acid oxidation and induces the transcription of oxidative phosphorylation genes by coactivating nuclear respiratory factors (NRF)-1 and -2, as well as mitochondrial transcription factor A (Tfam) [28]. Our results show that H9c2 cells demonstrate high ATP levels, mitochondrial mass and respiratory activity, as well as higher vulnerability to hypoxia and oxidative stress than HL-1 cells. Also, these cells exhibit higher levels of activated AMPK, but lower levels of PGC-1α, with elevated responses to hypoxia and the chemical AMPK activators metformin and A769662. Based on patterns of energy metabolism and sensitivity to hypoxia, we concluded that H9c2 cardioblastic cells could be a better model than HL-1 cells in the study of mechanisms of hypoxia and ischemia reperfusion injuries.

2. Materials and methods

2.1. Cell cultures

H9c2 embryonic rat heart-derived (ventricular) cells (myoblasts) from ATCC were cultured in Dulbecco's modified Eagle's medium (DMEM), supplemented with 10% fetal bovine serum (FBS) under 95% air/5% CO_2, and subcultured when at 50–60% confluence. Notably, a higher degree of confluence was associated with lower mitochondrial respiratory activity (data not shown). HL-1 cells from ATCC with cardiac phenotype were grown in fibronectin–gelatine coated flasks containing Claycomb medium ("Sigma") and supplemented with 10% FBS, 100 U/ml penicillin, 100 μg/ml streptomycin, 2 mM L-glutamine and 0.1 mM norepinephrine. Cells were cultured at 37 °C and 5% CO_2. Experiments were performed using cells between passages 10 and 14. Usually, new cultures were re-established from frozen stocks every three months.

2.2. Hypoxia-reoxygenation

H9c2 and HL-1 cells were subjected to different times of hypoxia (2–24 h) in a controlled hypoxic plastic chamber. In hypoxia experiments, nitrogen was flushed up to a partial oxygen pressure of about 0.4% and followed by 24 h of reoxygenation at 37 °C in some sets of experiments. To simulate ischemia, the cell culture medium for hypoxia was deprived of serum. Reoxygenation was conducted in a normoxic incubator at 37 °C by replacing the ischemic medium with normal culture medium supplemented with FBS. The time control group consisted of cells without the hypoxic stimulus kept in the reoxygenation buffer. Cell viability was assessed by the Trypan blue exclusion test.

2.3. Cellular respiration

Oxygen consumption of the cells was measured by high resolution respirometry [5,29] using a titration-injection respirometer (Oroboros® Oxygraph, Innsbruck, Austria) in culture

growth medium, before and after addition of the mitochondrial uncoupler carbonilcyanide p-triflouromethoxyphenylhydrazone (FCCP, 4 μM) at 37 °C, assuming an O_2 solubility of 10.5 μmol l^{-1} kPa^{-1} (1.4 μmol l^{-1} mm Hg^{-1}). DatLab software (Oroboros, Innsbruck, Austria) was used for data acquisition and analysis [5]. Respiration rates were expressed in pmol of O_2 per second per 10^6 cells. Both endogenous and uncoupled respiration rates were linearly dependent on the cell density, in the range of 0.1–6.0 × 10^6 cells/ml. Also, mitochondria-specific inhibitors blocked respiration, confirming that oxygen consumption was due to the mitochondrial respiratory chain (data not shown).

2.4. ATP levels

Cellular ATP content was measured using the bioluminescent somatic cell assay kit (Sigma) and multiplate luminometer [29]. After protein precipitation, ATP was extracted from cells using 0.5 M perchloric acid. Subsequent neutralization with 1 M KCO_3 and 100 mM HEPES was followed by centrifugation at 10,000 *g* for 5 min to remove precipitates. The ATP calibration curve was used for final analysis.

2.5. Citrate synthase activity

Cells were frozen in liquid nitrogen and stored at −80 ° C. The activity of the mitochondrial matrix marker enzyme citrate synthase (CS) was assayed spectrophotometrically by measuring coenzyme A formation at 412 nm, in cells at 30 ° C in the assay medium supplemented with 0.1% Triton X-100 as described previously [29].

2.6. SDS-PAGE and Western blotting

Tissue samples from mouse brain, heart atrium, and left ventricle were homogenized on ice in the lysis buffer containing 50 mM Tris–HCl, 150 mM NaCl, 0.02% sodium azide, 0.1% SDS, 1.0% NP-40, 0.5% sodium deoxycholate, 10 mM sodium orthophosphate, 25 mM glycero-2-phosphate, 25 mM NaF, pH 8.0, and supplemented with 1 mM PMSF, 0.2 mM Na-orthovanadate and proteinase inhibitor cocktail (“Calbiochem”). Insoluble material was removed by centrifugation at 4 °C, and protein concentration was determined in the supernatant using the BCA-Assay (Pierce) with bovine serum albumin as standard.

Cells (HL-1 and H9c2) were washed twice in phosphate-buffered saline (PBS) without calcium and magnesium. Equal numbers of cells were lysed by direct addition of protein sample buffer containing 60 mM Tris–HCl, 10% (wt/vol) glycerin, 3% sodium dodecyl sulfate (wt/vol), 5% 2-mercaptoethanol (wt/vol), and 0.05% (wt/vol) bromphenol blue, pH 6.8 and boiled at 100 °C for 5 min. Cell extracts were separated on a 10% sodium dodecyl sulfate-polyacrylamide gel and transferred to a nitrocellulose membrane in blotting buffer, containing 25 mM Tris (pH 8), 190 mM glycine, and 20% methanol, using a tank blot procedure. Blotting was performed at 400 mA for 60 min at 4 °C. The membrane was blocked for 1 h in TBS supplemented with 0.05% Tween 20 (vol/vol) and 5% (wt/vol) nonfat dry milk (“Sigma-Aldrich”). Incubation with the primary antibody against murine beta-tubulin II (Abcam), appropriately diluted in TBS supplemented with 0.05% Tween 20 (vol/vol) and 5% (wt/vol) dry milk powder, was carried out either at room temperature or overnight at 4 °C. After three washes (10 min each) with TBS containing 0.05% Tween 20 (wt/vol), the blot was incubated with the appropriate (anti-rabbit) horseradish peroxidase-

linked (rb-HRP) secondary antibody (“Sigma-Aldrich”), diluted 1:3000 in TBS supplemented with 0.05% Tween 20 (vol/vol) and 1.6% (wt/vol) dry milk powder for 45 min at room temperature. Following three washes, the bands were visualized using the enhanced chemiluminescence detection system (ECL, “Amersham”).

2.7. Mitochondrial morphology and structural arrangement

Cells were placed in Lab-Tek chambered coverglass (Nalge Nunc, Rochester, NY) with chamber volumes of 0.3 ml (~50×10^3 cells per chamber). In order to analyze the mitochondrial arrangement of H9c2 and HL-1 cells, cells were incubated for 30 min at room temperature with 50 nM tetramethylrodamine methyl ester (TMRM, “Sigma”). TMRM fluorescence was excited with a 543-nm helium–neon laser, at a laser output power of 1 mW. The TMRM signal was redirected to a 560-nm long-pass filter and collected in a pinhole (one Airy disk unit). TMRM fluorescence was fully colocalized with mitochondrial flavoproteins, integral components of the mitochondrial inner membrane (*data not shown*), and mitochondria-specific probe MitoTracker (“Molecular Probes”).

2.8. Immunofluorescence analysis

Cells were placed in chambered cover slides for 24 h ($5–10 \times 10^4$ cells per chamber), fixed with 4% PFA for 15 min at room temperature, washed 3 times with PBS, and permeabilized with 0.1% Triton X-100 for 10 min at 4 °C. Cells were washed once with PBS and blocked with 1% BSA in PBS for 1 h at room temperature. Immunostaining using primary antibodies against beta-tubulin II (“Abcam”, Novus Biochemicals) was performed overnight at 4 °C. After three washes with PBS, secondary antibodies (goat anti-mouse IgG Alexa Fluor 568 or goat anti-mouse IgG FITC) were added and incubated for 1 h at room temperature. In experiments with co-staining, cells were incubated with 200 nM MitoTracker red (“Molecular Probes” Inc., Leiden, Netherlands) for 30 min at 37 °C, prior to fixation for visualization of mitochondria.

2.9. Statistical analysis

Data are presented as means ± SD. The statistical differences between groups were calculated by two-tailed Student’s *t*-test. Differences were considered to be statistically significant when $P < 0.05$.

3. Results

3.1. Mitochondrial morphology

Our study analyzed mitochondrial morphology and structural arrangement in HL-1 and H9c2 cells, using the mitochondria-specific fluorescent dyes, TMRM and MitoTtracker (Fig. 1). Confocal fluorescent imaging demonstrated relatively more fragmented (punctuated) mitochondria in H9c2 cells. We also observed clusters or long threads of mitochondria surrounding nuclei, which may indicate a higher degree of mitochondrial networking in HL-1 cells (arrow in Fig. 1).

Previous studies proposed that mitochondrial interactions with the cytoskeleton, in particular, with the cytoskeletal protein beta-tubulin II, played a crucial role in the regulation

of cardiac energy metabolism [30–32]. Therefore, we assessed the subcellular localization of beta-tubulin II in H9c2 and HL-1 cells. Confocal immune-fluorescent analysis of fixed cells revealed a remarkable difference between H9c2 and HL-1 cell lines; beta-tubulin II was clearly present in H9c2 cells and, in contrast, absent in HL-1 cells (Fig. 2AB). Cells that exhibit an absence of beta-tubulin II have a different mode of regulation of mitochondrial respiratory functions than adult primary cardiomyocytes or myocardial tissue; differences exist with regard to patterns of energy metabolism, apparent Km for ADP, creatine and glucose stimulatory effects, etc. [24,25]. Hence, these studies propose that the interaction of mitochondria with beta-tubulin II plays a key role in the regulation of energy metabolism in the heart [30–32]. The absence of beta-tubulin II in HL-1 cells can also be explained by the cancerous phenotype of HL-1 cells. They are derived from the AT-1 mouse atrial cardiomyocyte tumor lineage, and perhaps rely mostly on cytoplasmic sources of ATP (glycolysis), rather than mitochondria-generated ATP. In our study, beta-tubulin II did not colocalize with mitochondria (Fig. 2C) in H9c2 cells, although a close localization of mitochondrial threads and beta-tubulin II filaments was seen in some regions (arrows in Fig. 2C).

Confocal imaging data were confirmed by protein analysis of beta-tubulin II in various cells and tissues (Fig. 3). The analysis demonstrates that beta-tubulin II was found in the brain, cardiac tissues (atrium and ventricle), smooth muscle cells (SMC), human umbilical vein endothelial cells (HUVEC), and H9c2 cardiomyoblasts. In contrast, human colon carcinoma DLD-1 cells demonstrated an absence of beta-tubulin II, and only small traces of the protein were observed in HL-1 cells.

Thus, these data demonstrate that H9c2 and HL-1 cells have distinct mitochondrial morphologies and structural arrangements. The presence of beta-tubulin II in H9c2 cells indicates that these cells are biochemically/ bioenergetically more similar to primary cardiomyocytes.

3.2. Cellular ATP levels and mitochondrial bioenergetics

In the next set of experiments, we assessed whether any differences existed between H9c2 and HL-1 with regard to cellular ATP levels, respiratory function of mitochondria and mitochondrial mass (content), evidenced by mitochondrial marker CS. As shown in Fig. 4A, ATP levels and activity of CS, an indicator of mitochondrial mass, were more than 2-fold higher in H9c2 cells compared to HL-1 cells. Likewise, H9c2 cells are characterized by significantly better respiratory function than HL-1 cells, as evidenced by both higher cellular endogenous respiration and uncoupled respiration (Fig. 4B). The uncoupling was performed by step-wise increasing concentration of mitochondrial uncoupler FCCP (1–5 μM). The uncoupled control ratio, calculated as the ratio of endogenous respiration to uncoupled respiration, was also higher in H9c2 cells than in HL-1 cells. Thus, these data indicate that ATP levels, mitochondrial respiration rates and mitochondrial mass are all significantly higher in H9c2 cardiomyoblasts than in HL-1 cells.

3.3. The effects of hypoxia-reoxygenation

Next, we studied the vulnerability of HL-1 and H9c2 cells to hypoxia and hypoxia-reoxygenation-induced oxidative stress by determining cell viability and respiration of mitochondria. Analysis of cell viability demonstrated that H9c2 cells are more sensitive to hypoxia-reoxygenation injury than HL-1 cells (Fig. 5A–D). Cell viability of H9c2 cells was 28% ($P < 0.05$) and 32% ($P < 0.001$) less than HL-1 cells at 16 h and 24 h after hypoxia, respectively (Fig. 5E). The cells exposed to hypoxia-reoxygenation exhibited distinct levels of mitochondrial dysfunction responses in a time-dependent manner. Mitochondrial respiratory function was relatively stable in HL-1 cells, whereas it was significantly diminished in H9c2 cells after 6 h, 12 h and 24 h of hypoxia and 24 h reoxygenation (Fig. 6). Notably, the results of mitochondrial dysfunction correlated with cell survival data. After 24 h of hypoxia and 24 h of reoxygenation, H9c2 and HL-1 cells displayed 64% and 95% cell viability and 58% and 90% mitochondrial respiration, respectively, compared to corresponding control cells. Thus, these data revealed that, in comparison to the HL-1 cells, H9c2 cells are highly sensitive to hypoxia and oxidative stress, which can be due to the high energy dependence (mitochondrial ATP) of these cells.

3.4. AMPK, and PGC-1α levels and effects of hypoxia-reoxygenation

AMPK and PGC-1α are two major signaling proteins in the regulation of energy metabolism and mitochondrial biogenesis and function. Their expression and activity in high energy consuming organs, like the heart, provide strict control over cardiac energy metabolism. Therefore, in the next series of experiments, we performed a comparative analysis of protein levels of AMPK, P-AMPK and PGC-1α in H9c2 and HL-1 cells, under control (normoxia) conditions, after hypoxia, and after hypoxia-reoxygenation. Analysis of energy metabolism and mitochondrial function (see 3.2.) revealed significant differences between H9c2 and HL-1 cells. We observed a significantly higher (about 3.2-fold) amount of phospho-AMPK and only slightly elevated levels of total AMPK in H9c2 cells compared to HL-1 cells (Fig. 7, red boxes). Interestingly, the PGC-1α level in H9c2 cells was lower than in HL-1 cells. To define the effects of hypoxia and oxidative stress on AMPK and PGC-1α, the cells were exposed to 2 h-hypoxia alone and 2 h-hypoxia with subsequent 24 h-reoxygenation. AMPK activators, the anti-diabetic drug metformin and a more specific compound A769662, were used as positive controls. As expected, short hypoxia (2 h) increased activation of AMPK (high P-AMPK level) in both H9c2 and HL-1 cells. Both cell types demonstrated similar responses (1.9-fold and 2.3-fold activation, respectively) to AMPK activation by hypoxia. Notably, in both cell types, a decline in the levels of P-AMPK was observed after 24 h of reoxygenation (Fig. 7A). Metformin had no effect on phosphorylation of AMPK at low concentration (1 mM) (Fig. 7B); however, pre-treatment of the cells with 4 mM metformin increased AMPK activation significantly. The effect was augmented (up to a 3-fold increase) by the specific activator A769662 (0.1 mM) (Fig. 7C). Overall, different protein levels of P-AMPK and PGC-1α were observed in H9c2 and HL-1 cells in response to normoxia and hypoxia.

4. Discussion

The present study is the first to demonstrate that i) H9c2 cardiomyoblasts remarkably differ from HL-1 cells with regard to energy metabolism; they contain higher cellular ATP levels, mitochondrial mass and respiration capacity than HL-1 cells, ii) protein contents of activated AMPK (P-AMPK) are higher, but PGC-1α expression is lower in H9c2 cells than in HL-1 cells, and iii) H9c2 cells are more sensitive to hypoxia and oxidative stress than HL-1 cells; they exhibit increased cell death and mitochondrial dysfunction after hypoxia-reoxygenation (features of H9c2 and HL-1 cells are summarized in the Table 1). Analysis of basal and uncoupled respiration of mitochondria revealed higher levels of mitochondrial function in H9c2 cells (Fig. 4B). Notably, elevated values were also observed in the uncoupling control ratio (ratio of FCCP stimulated and basal respiration), suggesting a higher degree of mitochondrial efficiency in H9c2 cells compared with HL-1 cells. This can be explained. Firstly, HL-1 cells are adult immortalized atrial cells, whereas ventricular H9c2 cells have an embryonic origin. Secondly, although HL-1 cells are used to develop a heart-specific phenotype in vitro [15], they are derived from mouse atrium, whereas H9c2 cells are derived from the rat left ventricle. Furthermore, although HL-1 cells may proliferate and contract (though we used non-beating HL-1 cells), H9c2 cells are undifferentiated myoblasts. Although both cell lines possess a number of disadvantages, they are the only cell lines able to substitute primary cardiomyocytes in in vitro models of IR injury and other cardiac diseases. It is difficult to rationalize their validity, which depends on the research focus. Several previous studies used HL-1 cells to investigate the cardiologic effects of physiological and pathological conditions in vitro, including oxidative stress, ischemia, hypoxia, hyperglycemia and hyperinsulinemia [33]. Similarly, H9c2 cells were widely used to study the effects, mechanisms, and therapeutic interventions of hypoxia/reoxygenation, autophagy, hypertrophy, insulin resistance, apoptosis, endoplasmic reticulum-mitochondria interactions and cellular signaling [6,13,14,16,34–36], as well as various differentiation aspects [37–39].

Our study demonstrates that the H9c2 cell model is more relevant than the HL-1 cell model in the mimicking of IR injury for studies of energy metabolism and mitochondrial function in the intact heart. Ventricular cardiomyocytes have a higher content of mitochondria than atrial cardiomyocytes, higher citrate synthase activity, more organized regulation, higher oxidative activity, greater ATP synthesis, and greater efficiency of energy transfer, including phosphocreatine shuttling [40–42]. Although HL-1 cells are able to contract, some cells lose this advantage after a few passages, and the increasing number of non-beating cells, which have different metabolic profiles, compromises the study and affects final results. We employed non-beating HL-1 cells in our study. Comparative analysis of primary adult cardiomyocytes and HL-1 cells revealed a dramatic difference in the mechanisms of mitochondrial ATP synthesis regulation, and apparent Km for ADP in primary cardiomyocytes was about 10 fold higher than in HL-1 cells [24,25]. Furthermore, the use of glucose as a major energy substrate by HL-1 cells is explained by the fact that they are cancerous cells. High levels of hexokinase were previously observed in HL-1 cells, indicating a glycolytic phenotype of energy metabolism, a common characteristic of cancer cells (Warburg effect). The Warburg effect postulates a defect in respiration and

mitochondrial oxidative phosphorylation together with increased aerobic glycolysis in tumor cells. Lack of β-tubulin class II and mitochondrial creatine kinase may be considered as a structural basis of the Warburg effect, where high activity of mitochondria-bound hexokinase 2 allows a direct utilization of mitochondrial ATP for glucose phosphorylation and lactate production [40,41]. Most likely, the Warburg effect is the main cause of the high dependence of HL-1 cells on glucose. H9c2 cell are derived from embryonic rat cardiomyocytes; however, they are not cancerous cells. This is confirmed, in addition to mitochondrial function, by morphological features and structural arrangements of mitochondria that are different in H9c2 and HL-1 cells (Fig. 1). Confocal fluorescent imaging discovered a higher number of mitochondria in H9c2 and a more branched network in some regions of HL-1 cells. Importantly, electrically non-connected, distinct mitochondria are a characteristic feature of primary cardiomyocytes, whereas the organization of mitochondria as a branched network is more typical in cancerous cells [24,30].

Previous findings strongly support the hypothesis that cytoskeletal elements interact with mitochondria to control mitochondrial respiration [32,42,43]. Primary adult cardiomyocytes and myocardial fibers demonstrated the regular arrangement of beta-tubulin II, fully co-localized with mitochondria, whereas other beta-tubulin isoforms (I, III and IV) were localized in the cytoplasm and differently organized in these cells [31]. Based on co-localization of beta-tubulin II with mitochondria, it was suggested that the cytoskeleton protein can directly interact with voltage dependent anion channel (VDAC) and, therefore, participate in the regulation of mitochondrial respiration. In contrast, HL-1 cells were characterized by the complete absence of beta-tubulin II. Our study confirmed this phenomenon by both confocal imaging and Western blot analysis, demonstrating almost complete absence of beta-tubulin II in HL-1 cells (Figs. 2 and 3). Like HL-1 cells, colon carcinoma DLD cells revealed no expression of beta-tubulin II, suggesting their similarity and cancerous phenotype (Fig. 3).

The heart is the most energy consuming organ, and mitochondria provide over 80% of the ATP required for adequate function of cardiomyocytes. These features make cardiomyocytes highly sensitive to hypoxia and oxidative stress induced by cardiac ischemia-reperfusion and myocardial infarction. In adult cardiomyocytes, hypoxia for 6 h or hypoxia followed by reoxygenation resulted in a 59% and 51% decrease in cellular viability, respectively [44]. The absence of oxygen blocks mitochondrial function, leading to energy and oxidative stresses and resulting in severe mitochondrial and organ tissue injury [7,45,46]. Our results revealed that H9c2 cells were significantly more sensitive to hypoxia-reoxygenation, demonstrating greater cell death and reduction in mitochondrial respiration. To the best of our knowledge, ours is the first study to provide comparative analysis of sensitivity of H9c2 and HL-1 cells to oxidative stress, although several studies examine the effects of hypoxia-reoxygenation in H9c2 or HL-1 cells individually [19,22,47].

Mitochondrial biogenesis is regulated by two major signaling molecules, AMPK and PGC-1α. At the same time, AMPK activation could markedly stimulate glucose uptake by increased translocation of GLUT4 to the plasma membrane [48,49], and also by elevated GLUT4 expression [50]. AMPK activation therefore serves to defend against energy

deficiency via activation of glucose transport and oxidation of fatty acids [27,51, 52]. Since H9c2 and HL-1 cells showed distinct mitochondrial respiration, mass and structural characteristics, we investigated expression of these proteins and observed that they demonstrated different patterns under normal and hypoxic conditions. High levels of activated AMPK in H9c2 cells were associated with higher functional activity, mitochondrial mass, and mitochondrial biogenesis, compared to HL-1 cells (Fig. 7). Growing evidence demonstrates that AMPK is also a critical regulator of mitochondrial biogenesis through activation of PGC-1α [28,53], an important regulator of transcription of many genes involved in mitochondrial energy metabolism [28] and mitochondrial physiology and oxidation of glucose and fatty acids. Despite high P-AMPK levels, mitochondrial mass and number, H9c2 cells contained significantly less PGC-1α compared to HL-1 cells. Mitochondrial biogenesis can be regulated both by PGC-1α-dependent and PGC-1α-independent mechanisms. Also, the higher activation of AMPK may be associated with the lower PGC-1α levels in H9c2 cells.

As for the PGC-1α-dependent pathway, we do not exclude the possibility that post-translational modification of existing PGC-1α proteins, independently of upregulation of the gene, may be sufficient to enhance mitochondrial biogenesis in H9c2 cells. Post-translational modifications through phosphorylation, acetylation, methylation, ubiquitination, and O-linked N-acetylglucosylation have been shown to affect the PGC-1α activity (*reviewed in* [54,55]. On the other hand, mitochondrial biogenesis (mass) can be regulated through PGC-1α-independent mechanisms. PGC-1α was not required for exercise-induced mitochondrial biogenesis in the mouse skeletal muscle [56], underlining the complexity of the role of PGC-1α in the regulation of mitochondrial biogenesis and respiratory function. In addition, PGC-1α mRNA expression was remarkably low in C2C12 myoblasts under basal conditions. Also, pyruvate-induced increase in mitochondrial biogenesis, mitochondrial protein expression, basal respiratory rate, and maximal oxidative capacity were independent of increases in PGC-1α and PGC-1β mRNA expression in C2C12 myoblasts [57]. Our data suggest that regulation of mitochondrial biogenesis in H9c2 cells, like in C2C12 myoblasts, is independent of PGC-1α, suggesting the existence of other pathways that regulate the oxidative capacity of mitochondria. The identification of the PGC-1α-independent pathways that regulate mitochondrial biogenesis will be of great interest in future.

Overall, these data clearly indicate that the AMPK and PGC-1α-associated regulatory program of mitochondrial biogenesis is rather different in HL-1 and H9c2 cells. In future, it would be interesting to investigate and compare AMPK-activated GLUT4 translocation, as well as troponin I levels in these cells. Since H9c2 cells represent myoblasts that are not yet differentiated into myotubes, it would also be interesting to compare energy metabolism, mitochondrial biogenesis, morphology, and function of H9c2 cells and primary adult cardiomyocytes.

5. Conclusion

H9c2 cells were found to be closer to normal primary cardiomyocytes with regard to their energy metabolism features. Like primary cardiomyocytes, they are more sensitive to

hypoxia than HL-1 cells and, therefore, can be more suitable in the design of the in vitro model of cardiac hypoxia-reoxygenation and myocardial infarction. Moreover, it is appropriate to utilize H9c2 cells to study the mechanisms of cardiac ischemia-reperfusion injury, to evaluate the efficiency of various therapeutic interventions, and in cardioplegic and organ preservation applications.

Acknowledgments

The research was funded by the Austrian Science Fund Grant P 22080-B20 (FWF) and the NHLBI National Institutes of Health Grant SC1HL118669 (SJ). The authors thank Bryan Agostini for his critical reading of the manuscript.

Abbreviations

AMPK	AMP-activated protein kinase
CS	citrate synthase
FBS	fetal bovine serum
FCCP	carbonilcyanide p-triflouromethoxyphenylhydrazone
IR	ischemia–reperfusion
PGC-1α	peroxisome proliferator-activated receptor gamma coactivator 1-alpha
TMRM	tetramethylrhodamine methyl ester

References

1. Aon MA, Cortassa S, Akar FG, O'Rourke B. Mitochondrial criticality: a new concept at the turning point of life or death. Biochim Biophys Acta. 2006; 1762:232–240. [PubMed: 16242921]
2. Balaban RS, Nemoto S, Finkel T. Mitochondria, oxidants, and aging. Cell. 2005; 120:483–495. [PubMed: 15734681]
3. Javadov S, Kuznetsov A. Mitochondrial permeability transition and cell death: the role of cyclophilin d. Front Physiol. 2013; 4:76. [PubMed: 23596421]
4. Kroemer G, Reed JC. Mitochondrial control of cell death. Nat Med. 2000; 6:513–519. [PubMed: 10802706]
5. Kuznetsov AV, Schneeberger S, Seiler R, Brandacher G, Mark W, Steurer W, Saks V, Usson Y, Margreiter R, Gnaiger E. Mitochondrial defects and heterogeneous cytochrome c release after cardiac cold ischemia and reperfusion. Am J Physiol Heart Circ Physiol. 2004; 286:H1633–H1641. [PubMed: 14693685]
6. Abas L, Bogoyevitch MA, Guppy M. Mitochondrial ATP production is necessary for activation of the extracellular-signal-regulated kinases during ischaemia/reperfusion in rat myocyte-derived H9c2 cells. Biochem J. 2000; 349:119–126. [PubMed: 10861219]
7. Turer AT, Hill JA. Pathogenesis of myocardial ischemia–reperfusion injury and rationale for therapy. Am J Cardiol. 2010; 106:360–368. [PubMed: 20643246]
8. Orita H, Fukasawa M, Hirooka S, Fukui K, Kohi M, Washio M. A cardiac myocyte culture system as an in vitro experimental model for the evaluation of hypothermic preservation. Surg Today. 1993; 23:439–443. [PubMed: 8324337]
9. Orita H, Fukasawa M, Hirooka S, Uchino H, Fukui K, Kohi M, Washio M. Cardiac myocyte functional and biochemical changes after hypothermic preservation in vitro. Protective effects of storage solutions. J Thorac Cardiovasc Surg. 1994; 107:226–232. [PubMed: 8283890]

10. Schmid T, Landry G, Fields BL, Belzer FO, Haworth RA, Southard JH. The use of myocytes as a model for developing successful heart preservation solutions. Transplantation. 1991; 52:20–26. [PubMed: 1907042]
11. Neary MT, Ng KE, Ludtmann MH, Hall AR, Piotrowska I, Ong SB, Hausenloy DJ, Mohun TJ, Abramov AY, Breckenridge RA. Hypoxia signaling controls postnatal changes in cardiac mitochondrial morphology and function. J Mol Cell Cardiol. 2014; 74C:340–352. [PubMed: 24984146]
12. Bonavita F, Stefanelli C, Giordano E, Columbaro M, Facchini A, Bonafe F, Caldarera CM, Guarnieri C. H9c2 cardiac myoblasts undergo apoptosis in a model of ischemia consisting of serum deprivation and hypoxia: inhibition by PMA. FEBS Lett. 2003; 536:85–91. [PubMed: 12586343]
13. Cao X, Wang X, Ling Y, Song X, Yang P, Liu Y, Liu L, Wang L, Guo J, Chen A. Comparison of the degree of autophagy in neonatal rat cardiomyocytes and H9c2 cells exposed to hypoxia/reoxygenation. Clin Lab. 2014; 60:809–814. [PubMed: 24839824]
14. Chang G, Zhang D, Liu J, Zhang P, Ye L, Lu K, Duan Q, Zheng A, Qin S. Exenatide protects against hypoxia/reoxygenation-induced apoptosis by improving mitochondrial function in H9c2 cells. Exp Biol Med. 2014; 239:414–422. (Maywood.).
15. Claycomb WC, Lanson NA Jr, Stallworth BS, Egeland DB, Delcarpio JB, Bahinski A, JIzzo N Jr. HL-1 cells: a cardiac muscle cell line that contracts and retains phenotypic characteristics of the adult cardiomyocyte. Proc Natl Acad Sci U S A. 1998; 95:2979–2984. [PubMed: 9501201]
16. Kolamunne RT, Clare M, Griffiths HR. Mitochondrial superoxide anion radicals mediate induction of apoptosis in cardiac myoblasts exposed to chronic hypoxia. Arch Biochem Biophys. 2011; 505:256–265. [PubMed: 20971059]
17. Prathapan A, Vineetha VP, Raghu KG. Protective effect of *Boerhaavia diffusa* L. against mitochondrial dysfunction in angiotensin II induced hypertrophy in H9c2 cardiomyoblast cells. PLoS ONE. 2014; 9:e96220. [PubMed: 24788441]
18. Shin EJ, Schram K, Zheng XL, Sweeney G. Leptin attenuates hypoxia/reoxygenation-induced activation of the intrinsic pathway of apoptosis in rat H9c2 cells. J Cell Physiol. 2009; 221:490–497. [PubMed: 19653255]
19. Sun L, Zhao M, Yu XJ, Wang H, He X, Liu JK, Zang WJ. Cardioprotection by acetylcholine: a novel mechanism via mitochondrial biogenesis and function involving the PGC-1alpha pathway. J Cell Physiol. 2013; 228:1238–1248. [PubMed: 23139024]
20. Teixeira G, Abrial M, Portier K, Chiari P, Couture-Lepetit E, Tourneur Y, Ovize M, Gharib A. Synergistic protective effect of cyclosporin A and rotenone against hypoxia-reoxygenation in cardiomyocytes. J Mol Cell Cardiol. 2013; 56:55–62. [PubMed: 23238221]
21. Milerova M, Charvatova Z, Skarka L, Ostadalova I, Drahota Z, Fialova M, Ostadal B. Neonatal cardiac mitochondria and ischemia/reperfusion injury. Mol Cell Biochem. 2010 Feb; 335(1–2): 147–153. [PubMed: 19756957]
22. Pelloux S, Robillard J, Ferrera R, Bilbaut A, Ojeda C, Saks V, Ovize M, Tourneur Y. Non-beating HL-1 cells for confocal microscopy: Application to mitochondrial functions during cardiac preconditioning. Prog Biophys Biophys Chem. 2006; 90:270–298.
23. Muscari C, Gamberini C, Bonafe' F, Giordano E, Bianchi C, Lenaz G, Caldarera CM. Evaluation of cellular energetics by the pasteur effect in intact cardiomyoblasts and isolated perfused hearts. Mol Cell Biochem. 2004; 258:91–97. [PubMed: 15030173]
24. Beraud N, Pelloux S, Kuznetsov A, Guzun R, Anmann T, Tourneur Y, Ojeda C, Saks V. Comparative bioeneregetics of isolated cardiomyocytes and HL-1 cells: mitochondrial dynamics, respiration regulation and creatine kinase expression. Biochim Biophys Acta Bioenerg. 2006:514–515.
25. Monge C, Beraud N, Tepp K, Pelloux S, Chahboun S, Kaambre T, Kadaja L, Roosimaa M, Piirsoo A, Tourneur Y, Kuznetsov AV, Saks V, Seppet E. Comparative analysis of the bioenergetics of adult cardiomyocytes and nonbeating HL-1 cells: respiratory chain activities, glycolytic enzyme profiles, and metabolic fluxes. Can J Physiol Pharmacol. 2009; 87:318–326. [PubMed: 19370085]

26. Seppet E, Paju K, Roosimaa M, Kadaja L, Peet N, Eimre M, Orlova E, Saks V. Distinct organization of energy metabolism in HL-1 cardiac cells and cardiomyocytes. J Mol Cell Cardiol. 2008; 44:780–781.
27. Hardie DG, Hawley SA, Scott JW. AMP-activated protein kinase—development of the energy sensor concept. J Physiol. 2006; 574:7–15. [PubMed: 16644800]
28. Wu Z, Puigserver P, Andersson U, Zhang C, Adelmant G, Mootha V, Troy A, Cinti S, Lowell B, Scarpulla RC, Spiegelman BM. Mechanisms controlling mitochondrial biogenesis and respiration through the thermogenic coactivator PGC-1. Cell. 1999; 98:115–124. [PubMed: 10412986]
29. Kuznetsov AV, Margreiter R, Amberger A, Saks V, Grimm M. Changes in mitochondrial redox state, membrane potential and calcium precede mitochondrial dysfunction in doxorubicin-induced cell death. Biochim Biophys Acta. 2011; 1813:1144–1152. [PubMed: 21406203]
30. Gonzalez-Granillo M, Grichine A, Guzun R, Usson Y, Tepp K, Chekulayev V, Shevchuk I, Karu-Varikmaa M, Kuznetsov AV, Grimm M, Saks V, Kaambre T. Studies of the role of tubulin beta II isotype in regulation of mitochondrial respiration in intracellular energetic units in cardiac cells. J Mol Cell Cardiol. 2012; 52:437–447. [PubMed: 21846472]
31. Guzun R, Karu-Varikmaa M, Gonzalez-Granillo M, Kuznetsov AV, Michel L, Cottet-Rousselle C, Saaremae M, Kaambre T, Metsis M, Grimm M, Auffray C, Saks V. Mitochondria-cytoskeleton interaction: distribution of beta-tubulins in cardiomyocytes and HL-1 cells. Biochim Biophys Acta. 2011; 1807:458–469. [PubMed: 21296049]
32. Kuznetsov AV, Javadov S, Guzun R, Grimm M, Saks V. Cytoskeleton and regulation of mitochondrial function: the role of beta-tubulin II. Front Physiol. 2013; 4:82. [PubMed: 23630499]
33. White SM, Constantin PE, Claycomb WC. Cardiac physiology at the cellular level: use of cultured HL-1 cardiomyocytes for studies of cardiac muscle cell structure and function. Am J Physiol Heart Circ Physiol. 2004; 286:H823–H829. [PubMed: 14766671]
34. Cao X, Chen A, Yang P, Song X, Liu Y, Li Z, Wang X, Wang L, Li Y. Alpha-lipoic acid protects cardiomyocytes against hypoxia/reoxygenation injury by inhibiting autophagy. Biochem Biophys Res Commun. 2013; 441:935–940. [PubMed: 24216106]
35. Kolamunne RT, Dias IH, Vernallis AB, Grant MM, Griffiths HR. Nrf2 activation supports cell survival during hypoxia and hypoxia/reoxygenation in cardiomyoblasts; the roles of reactive oxygen and nitrogen species. Redox Biol. 2013; 1:418–426. [PubMed: 24191235]
36. Neuzil J, Widen C, Gellert N, Swettenham E, Zobalova R, Dong LF, Wang XF, Lidebjer C, Dalen H, Headrick JP, Witting PK. Mitochondria transmit apoptosis signalling in cardiomyocyte-like cells and isolated hearts exposed to experimental ischemia–reperfusion injury. Redox Rep. 2007; 12:148–162. [PubMed: 17623522]
37. Pagano M, Naviglio S, Spina A, Chiosi E, Castoria G, Romano M, Sorrentino A, Illiano F, Illiano G. Differentiation of H9c2 cardiomyoblasts: the role of adenylate cyclase system. J Cell Physiol. 2004 Mar; 198(3):408–416. [PubMed: 14755546]
38. Ménard C, Pupier S, Mornet D, Kitzmann M, Nargeot J, Lory P. Modulation of L-type calcium channel expression during retinoic acid-induced differentiation of H9C2 cardiac cells. J Biol Chem. 1999 Oct 8; 274(41):29063–29070. [PubMed: 10506158]
39. Comelli M, Domenis R, Bisetto E, Contin M, Marchini M, Ortolani F, Tomasetig L, Mavelli I. Cardiac differentiation promotes mitochondria development and ameliorates oxidative capacity in H9c2 cardiomyoblasts. Mitochondrion. 2011 Mar; 11(2):315–326. [PubMed: 21147273]
40. Saks V, Guzun R, Timohhina N, Tepp K, Varikmaa M, Monge C, Beraud N, Kaambre T, Kuznetsov A, Kadaja L, Eimre M, Seppet E. Structure–function relationships in feedback regulation of energy fluxes in vivo in health and disease: mitochondrial interactosome. Biochim Biophys Acta. 2010; 1797:678–697. [PubMed: 20096261]
41. Guzun R, Timohhina N, Tepp K, Gonzalez-Granillo M, Shevchuk I, Chekulayev V, Kuznetsov AV, Kaambre T, Saks VA. Systems bioenergetics of creatine kinase networks: physiological roles of creatine and phosphocreatine in regulation of cardiac cell function. Amino Acids. 2011; 40:1333–1348. [PubMed: 21390528]
42. Appaix F, Kuznetsov AV, Usson Y, Kay L, Andrienko T, Olivares J, Kaambre T, Sikk P, Margreiter R, Saks V. Possible role of cytoskeleton in intracellular arrangement and regulation of mitochondria. Exp Physiol. 2003; 88:175–190. [PubMed: 12525866]

43. Capetanaki Y. Desmin cytoskeleton: a potential regulator of muscle mitochondrial behavior and function. Trends Cardiovasc Med. 2002; 12:339–348. [PubMed: 12536120]
44. Kang PM, Haunstetter A, Aoki H, Usheva A, Izumo S. Morphological and molecular characterization of adult cardiomyocyte apoptosis during hypoxia and reoxygenation. Circ Res. 2000; 87:118–125. [PubMed: 10903995]
45. Kay L, Rossi A, Saks V. Detection of early ischemic damage by analysis of mitochondrial function in skinned fibers. Mol Cell Biochem. 1997; 174:79–85. [PubMed: 9309669]
46. Sun CN, Dhalla NS, Olson RE. Formation of gigantic mitochondria in hypoxic isolated perfused rat hearts. Experientia. 1969; 25:763–764. [PubMed: 5809311]
47. Sun L, Isaak CK, Zhou Y, Petkau JC, Liu OKY, Siow YL. Salidroside and tyrosol from Rhodiola protect H9c2 cells from ischemia/reperfusion-induced apoptosis. Life Sci. 2012; 91:151–158. [PubMed: 22771701]
48. Carling D. The AMP-activated protein kinase cascade—a unifying system for energy control. Trends Biochem Sci. 2004; 29:18–24. [PubMed: 14729328]
49. Kurth-Kraczek EJ, Hirshman MF, Goodyear LJ, Winder WW. 5′ AMP-activated protein kinase activation causes GLUT4 translocation in skeletal muscle. Diabetes. 1999; 48(8):1667–1671. [PubMed: 10426389]
50. Zheng D, MacLean PS, Pohnert SC, Knight JB, Olson AL, Winder WW, Dohm GL. Regulation of muscle GLUT-4 transcription by AMP-activated protein kinase. J Appl Physiol. 2001; 91(3): 1073–1083. [PubMed: 11509501]
51. Russel RR III, Bergeron GI, Young Shulman LH. Translocation of myocardial GLUT-4 and increased glucose uptake through activation of AMPK by AICAR. Am J Physiol. 1999; 277(2):H643–649. [PubMed: 10444490]
52. Holmes BF, Kurth-Kraczek EJ, Winder WW. Chronic activation of 5′-AMP-activated protein kinase increases GLUT-4, hexokinase, and glycogen in muscle. J Appl Physiol. 1999; 87:1990–1995. [PubMed: 10562646]
53. Jager S, Handschin C, St-Pierre J, Spiegelman BM. AMP-activated protein kinase (AMPK) action in skeletal muscle via direct phosphorylation of PGC-1alpha. Proc Natl Acad Sci U S A. 2007; 104:12017–12022. [PubMed: 17609368]
54. Fernandez-Marcos PJ, Auwerx J. Regulation of PGC-1alpha, a nodal regulator of mitochondrial biogenesis. Am J Clin Nutr. 2011; 93:884S–8890S. [PubMed: 21289221]
55. Jeninga EH, Schoonjans K, Auwerx J. Reversible acetylation of PGC-1: connecting energy sensors and effectors to guarantee metabolic flexibility. Oncogene. 2010; 29:4617–4624. [PubMed: 20531298]
56. Rowe GC, El-Khoury R, Patten IS, Rustin P, Arany Z. PGC-1alpha is dispensable for exercise-induced mitochondrial biogenesis in skeletal muscle. PLoS ONE. 2012; 7:e41817. [PubMed: 22848618]
57. Wilson L, Yang Q, Szustakowski JD, Gullicksen PS, Halse R. Pyruvate induces mitochondrial biogenesis by a PGC-1 alpha-independent mechanism. Am J Physiol Cell Physiol. 2007; 292:C1599–C1605. [PubMed: 17182725]

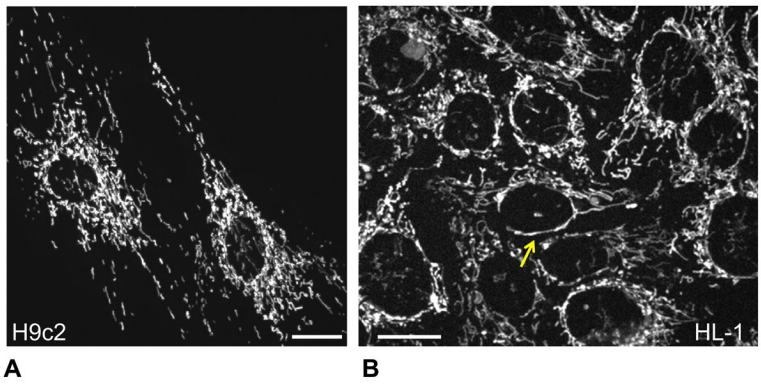

Fig. 1.

Different mitochondrial organization/arrangement in H9c2 and HL-1 cells. Representative confocal imaging of mitochondrial organization in H9c2 (A) and HL-1 (B) cells demonstrate punctuated/distinct mitochondria in H9c2 cells (visible also in adult primary cardiomyocytes) and more mitochondrial network in HL-1 cells more typical for various cancerous cells. Mitochondria were visualized by fluorescent confocal microscopy using mitochondrial specific probe TMRM (0.1 μM, see Methods). Bar, 20 μm.

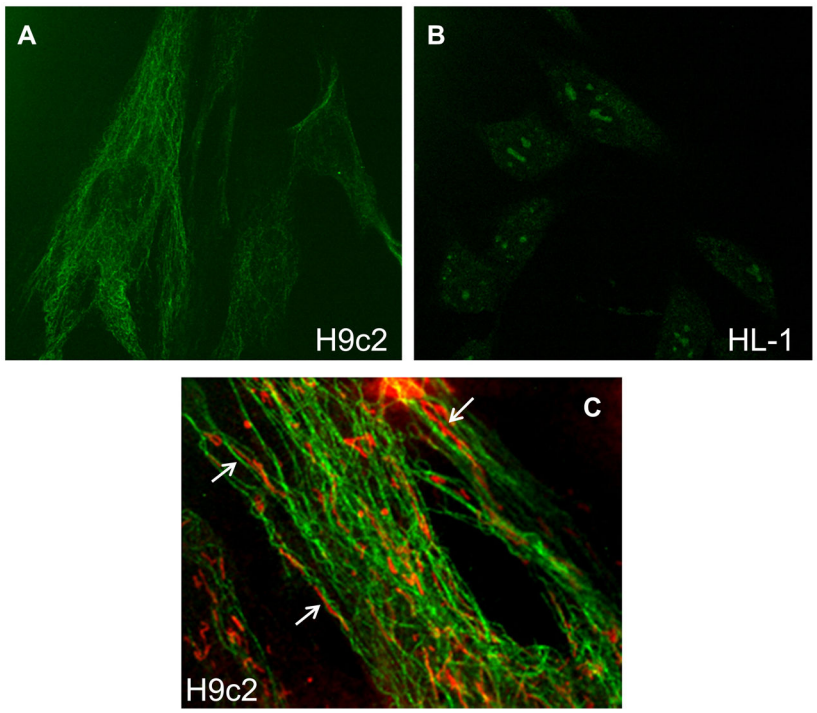

Fig. 2.

Confocal imaging of beta-tubulin II in H9c2 and HL-1 cells. Cells were fixed and stained with antibodies against beta-tubulin II as described in Methods, using second antibodies Fluoro-Nanogold-anti-mouse Fab′ antibodies bound to Alexa-Fluor-488. A: Note the presence of beta-tubulin II in H9c2 cells and absence in HL-1 cells (B). C: H9c2 cells were stained with antibodies against beta-tubulin II (green) and additionally with MitoTracker red for visualization of mitochondria. In some regions, a close arrangement of mitochondrial threads and tubulin filaments can be seen (arrows).

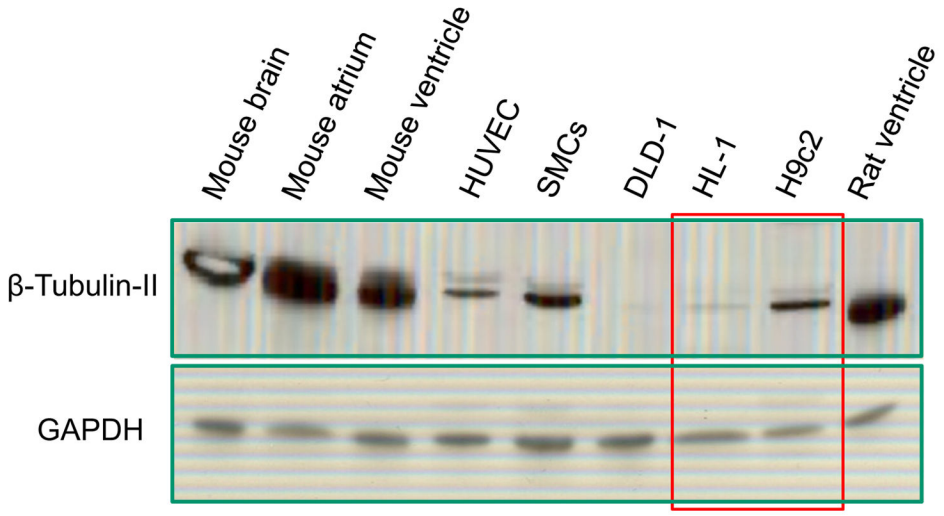

Fig. 3.

Western blot analysis of beta-tubulin II in various cells and tissues. Similarly to confirming the results of fluorescent confocal imaging (see Fig. 2), the presence of beta-tubulin II in H9c2 cells and the absence in HL-1 cells were found. Note the abundant amount of beta-tubulin II in rat and mice heart and in brain. All probes contained app. 20 μg of total protein. GAPDH ("Ambion") was used a loading control. DLD, human colorectal carcinoma cells; HUVEC, human umbilical vein endothelial cells; SMS, smooth muscle cells.

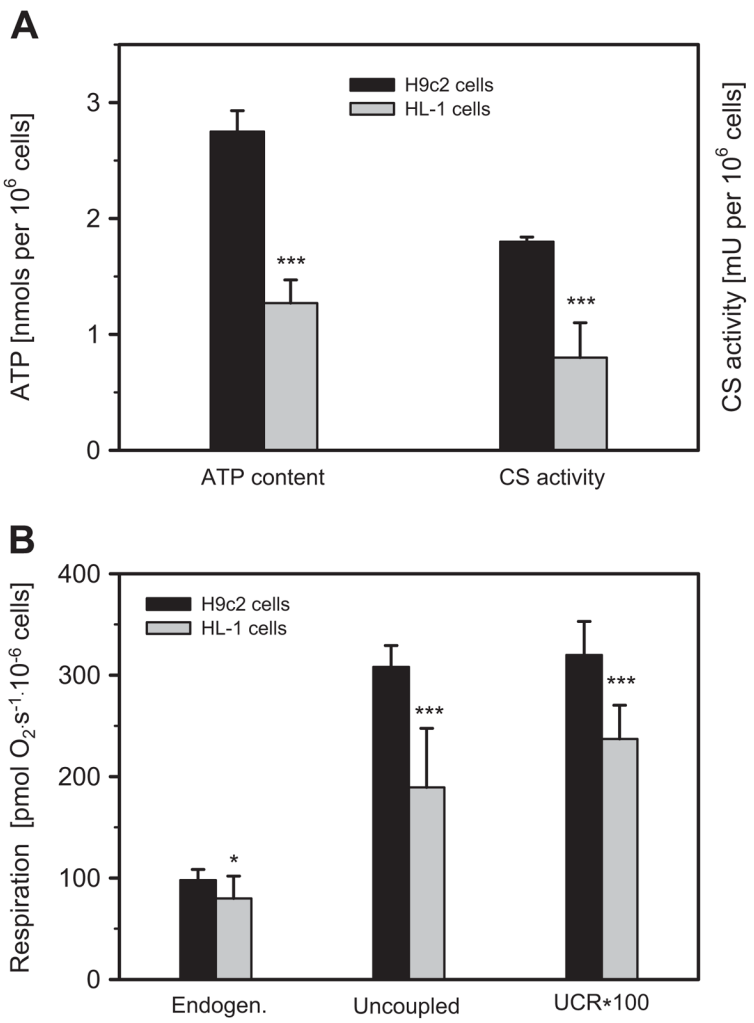

Fig. 4.

Biochemical, bioenergetic properties and respiratory activities are different in H9c2 and HL-1 cells. A: H9c2 cells demonstrate significantly higher level of ATP (per 10^6 cells) and activity of mitochondrial marker enzyme citrate synthase (CS) as compared with HL-1 cells. B: Both endogenous and uncoupled (by FCCP) respiration, as well as uncoupled control ratio (UCR) are significantly higher in H9c2 cells than in HL-1 cells ($N = 3$; * $P < 0.05$; *** $P < 0.001$).

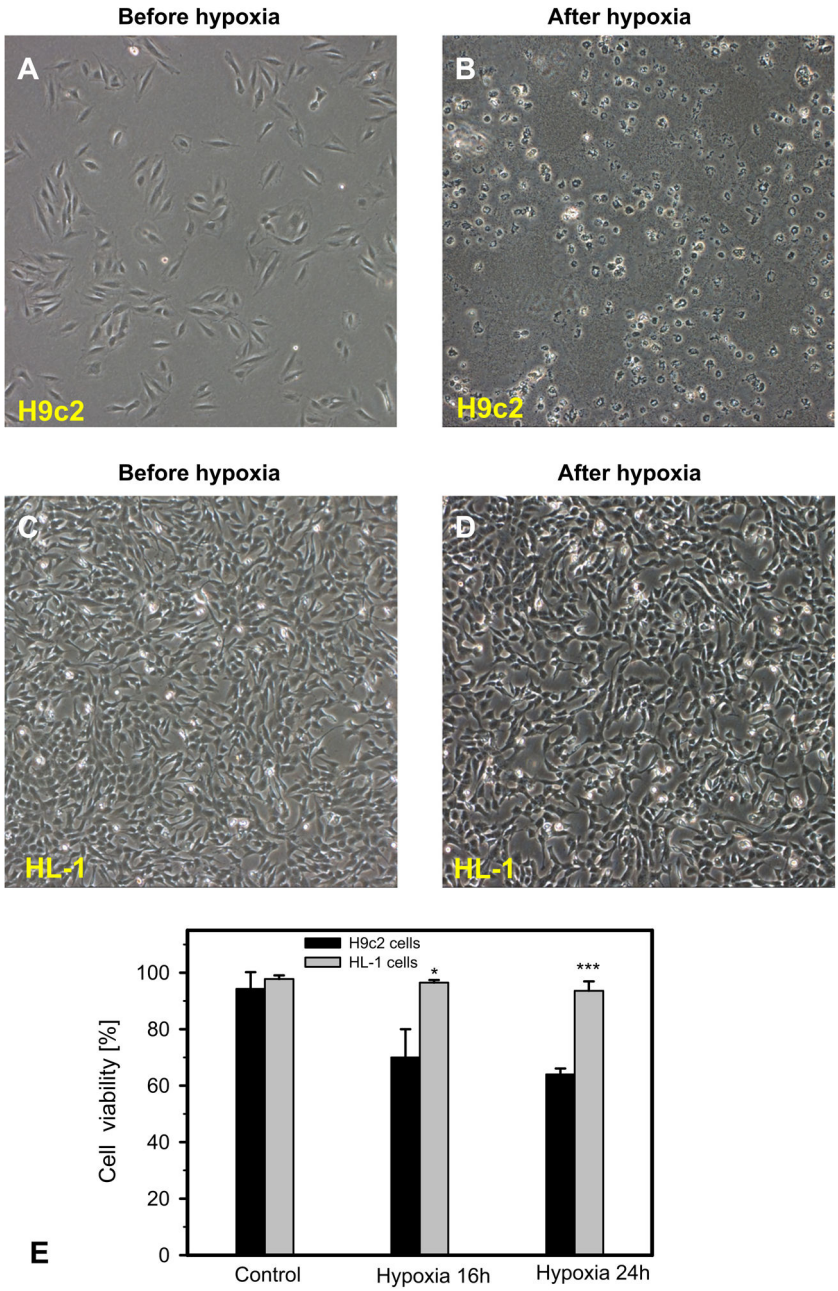

Fig. 5.

Increased sensitivity of H9c2 cells to hypoxia compared to HL-1 cells. A–D: Representative phase contrast microscopy of H9c2 and HL-1 cells. Representative phase contrast pictures were taken before (A, C) and after (B, D) hypoxic treatment (0. 4% oxygen) for 16 h and reoxygenation for 24 h. H9c2 cells were almost completely lysed after hypoxia, whereas HL-1 substantially survived after the same hypoxic regime. HL-1 and H9c2 cells were seeded in 6-well plates and grown overnight under their corresponding conditions. E: Quantitative data of cell viability after 16 h and 24 h of hypoxia. $N = 3$; * $P < 0.05$; *** $P < 0.001$.

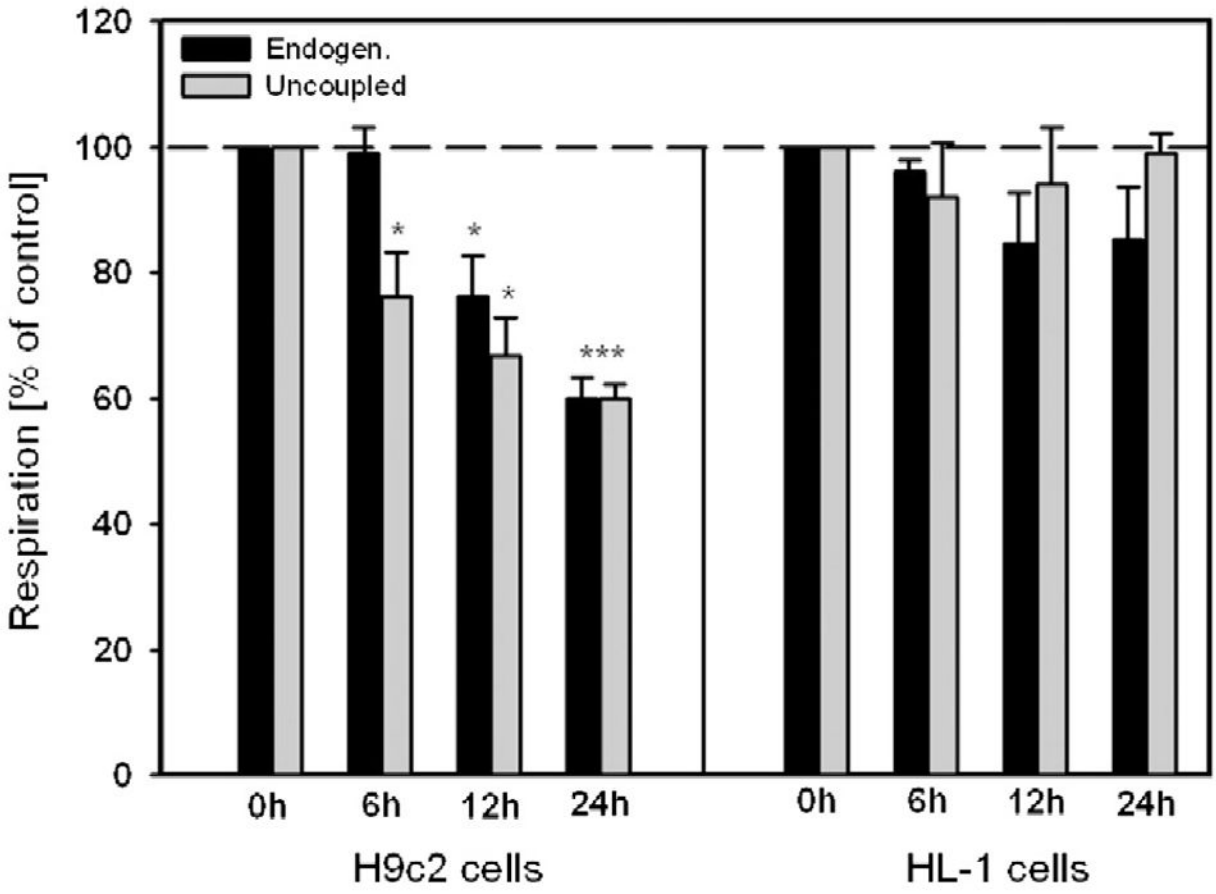

Fig. 6.

Mitochondrial respiratory parameters of H9c2 and HL-1 cells after hypoxia-reoxygenation. Basal and FCCP-uncoupled respiration at 6 h, 12 h and 24 h after hypoxia and standard time (2 h) of reoxygenation. In contrast to HL-1 cells (which demonstrate a stability), H9c2 cells show significant decrease (up to 60% of control in respiration rates after 24 h of hypoxia). $N = 3$; * $P < 0.05$; *** $P < 0.001$.

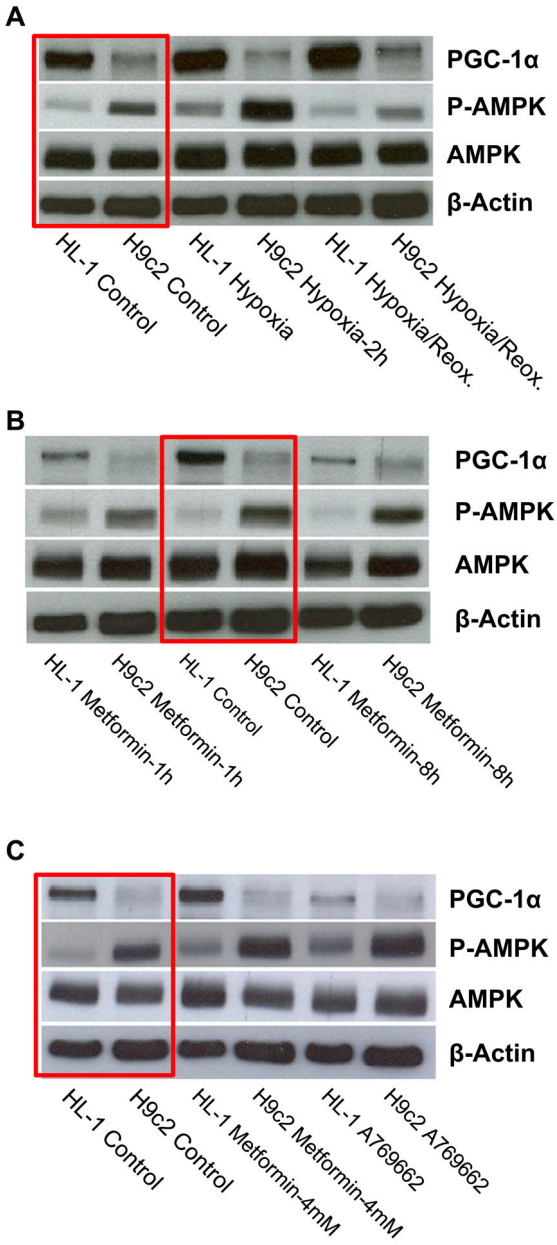

Fig. 7.

Comparative Western blot analysis of AMPK, P-AMPK, and PGC-1α in H9c2 and HL-1 cells. A–C: Whereas a similar level of AMPK was found in both cell lines, H9c2 cells demonstrate significantly higher amount of phospho-AMPK (activated, P-AMPK). In contrast, higher level of PGC-1α was found in HL-1 cells as compared with H9c2 cells. A: Short hypoxia (2 h) resulted in significant activation of AMPK to P-AMPK, both in H9c2 and in HL-1 cells. B: Treatment with 1 mM of activator of AMPK metformin had no effect. C: Treatment with higher (4 mM) concentration of metformin showed an activation of AMPK, more visible after treatment with specific activator A769662 (0.1 mM, 8 h).

Table 1

Metabolic, biochemical, bioenergetic and morphological differences between rat H9c2 ventricle and mouse HL-1 atrial cells with cardiac phenotype.

Parameter/criteria	H9c2 cardiomyoblasts	HL-1 cells
Citrate synthase (CS)[a] Mitochondrial marker	↑	↓
ATP content[a] Cellular energy status	↑	↓
Cellular/mitochondrial State 3 maximal respiration	↑	↓
Uncoupled respiration	↑	↓
Uncoupled control ratio (UCR)	↑	↓
Mitochondrial morphology Discrete mitochondria	↑	↓
Mitochondrial morphology Mitochondrial network	↓	↑
Tubulin beta-II (mitochondrial isotype)	+	--
Sensitivity to hypoxia-reoxygenation	↑	↓
Phospho-AMP activated protein kinase (pAMPK)	↑	↓
PGC-1α	↓	↑

[a]Calculated per 10^6 cells.